

## REPORT DOCUMENTATION PAGE

Form Approved

OMB No. 0704-0168

This document contains neither recommendations nor conclusions of the Defense Advanced Research Projects Agency. It has been approved for public release by the Defense Advanced Research Projects Agency. Distribution outside the agency is controlled by the Defense Technical Information Center.			
1. AGENCY USE ONLY (Leave Blank)	2. REPORT DATE	3. REPORT TYPE	4. DATES COVERED
	January 12, 1996	Tech Rpt. # 27	
4. TITLE AND SUBTITLE Crystal Structure, Electric and Magnetic Behavior of Ce <sub>2</sub> Pd <sub>9</sub> Sb <sub>3</sub>		5. FUNDING NUMBERS N00014-93-1-0904	
6. AUTHOR(S) R.A. Gordon, F.J. DiSalvo, R. Pottgen and N.E. Brese		Dr. John Pazik R&T: 3134037ess08	
7. PERFORMING ORGANIZATION NAME(S) AND ADDRESS(ES) Department of Chemistry Cornell University Ithaca, NY 14853-1301		8. PERFORMING ORGANIZATION REPORT NUMBER	
9. SPONSORING/MONITORING AGENCY NAME(S) AND ADDRESS(ES) Office of Naval Research Chemistry Program 800 N. Quincy St. Alexandria, VA 22217		10. SPONSORING/MONITORING AGENCY REPORT NUMBER	
11. SUPPLEMENTARY NOTES			
12a. DISTRIBUTION/AVAILABILITY STATEMENT This document has been approved for public release and sale; its distribution is unlimited		12b. DISTRIBUTION CODE	
13. ABSTRACT (Maximum 200 words) A new ternary compound in the Ce-Pd-Sb system has been observed and studied by single crystal diffraction, magnetic susceptibility and resistivity. This new compound, Ce <sub>2</sub> Pd <sub>9</sub> Sb <sub>3</sub> , was determined to crystallize in the Y <sub>2</sub> Co <sub>3</sub> Ga <sub>9</sub> structure type: Cmcm, a=13.769(2) Å, b=8.0412(8) Å, c=9.348(1) Å, wR2=6.7%, 709 F <sup>2</sup> values, and 42 variables. An anti-site relationship exists between the p-block and transition elements relative to the parent structure type. The magnetic susceptibility exhibits Curie-Weiss behavior with an effective cerium moment of 2.51(3) μB, comparable to the free ion value of 2.54 μB, and negligible exchange (θ=2(2)K). No ordering of moments is observed above 4.2K. Resistivity measurements indicate simple metallic behavior with no apparent evidence for interaction between the local cerium moments and conduction electrons.			
14. SUBJECT TERMS  19960206 086		15. NUMBER OF PAGES 20	
		16. PRICE CODE	
17. SECURITY CLASSIFICATION OF REPORT Unclassified	18. SECURITY CLASSIFICATION OF THIS PAGE Unclassified	19. SECURITY CLASSIFICATION OF ABSTRACT Unclassified	20. LIMITATION OF ABSTRACT

NSN 7540-31-280-5500

Standard Form 298 (Rev. 2-89)  
Prescribed by ANSI Std Z39-18  
298-102

**OFFICE OF NAVAL RESEARCH**

Grant or Contract N00014-93-1-0904

R&T Code 3134037ess08  
Scientific Officer: Dr. John Pazik

Technical Report No. 27

"Crystal Structure, Electric and Magnetic Behavior of Ce<sub>2</sub>Pd<sub>9</sub>Sb<sub>3</sub>"

by

R.A. Gordon, F.J. DiSalvo, R. Pottgen and N.E. Brese

Submitted to

Faraday Transactions

Cornell University  
Department of Chemistry  
Ithaca, NY 14853

January 12, 1996

Reproduction in whole or in part is permitted for any purpose  
of the United States Government

This document has been approved for public release  
and sale; its distribution is unlimited

Draft  
Submitted  
10/13/95

Corresponding author:

F.J. DiSalvo

Department of Chemistry, Cornell University, Ithaca, NY 14853, USA

## Crystal Structure, Electric and Magnetic Behavior of $\text{Ce}_2\text{Pd}_9\text{Sb}_3$

Robert. A. Gordon and Francis. J. DiSalvo

*Department of Chemistry,  
Cornell University, Ithaca, NY 14853, USA*

Rainer Pöttgen

*Max-Planck-Institut für Festkörperforschung  
Heisenbergstrasse 1, D-70569 Stuttgart, Germany*

Nathaniel. E. Brese

*Osram Sylvania Inc.  
Hawes Street, Towanda PA 18848, USA*

To be submitted to Faraday Transactions

---

### Abstract

A new ternary compound in the Ce-Pd-Sb system has been observed and studied by single crystal diffraction, magnetic susceptibility and resistivity. This new compound,  $\text{Ce}_2\text{Pd}_9\text{Sb}_3$ , was determined to crystallize in the  $\text{Y}_2\text{Co}_3\text{Ga}_9$  structure type: Cmcm,  $a = 13.769(2)\text{\AA}$ ,  $b = 8.0412(8)\text{\AA}$ ,  $c = 9.348(1)\text{\AA}$ ,  $wR2 = 6.7\%$ , 709  $F^2$  values, and 42 variables. An anti-site relationship exists between the p-block and transition elements relative to the parent structure type. The magnetic susceptibility exhibits Curie-Weiss behavior with an effective cerium moment of  $2.51(3)\mu_B$ , comparable to the free ion value of  $2.54\mu_B$ , and negligible exchange ( $\theta = 2(2)\text{K}$ ). No ordering of moments is observed above 4.2K. Resistivity measurements indicate simple metallic behavior with no apparent evidence for interaction between the local cerium moments and conduction electrons.

---

## **Introduction**

Typically, the 4f electrons of rare earth elements in intermetallic compounds are well-localized, but the f-states are split by a weak crystal field due to the near-neighbour environment, and weak, inter-lanthanide exchange can occur through polarization of conduction electrons around the local moment. In some cases, however, and for cerium intermetallics in particular, hybridization can occur between the 4f states and conduction states, leading to some interesting electronic effects such as intermediate valence or heavy fermion behavior<sup>1,2</sup>.

As part of our studies of cerium intermetallics<sup>3-6</sup> and the interplay between their structures and physical properties, we have been examining the palladium-rich region of the Ce-Pd-Sb phase diagram. Already known to exist in this phase diagram are the ternary compounds CePdSb<sup>7</sup>, CePd<sub>2</sub>Sb<sub>2</sub><sup>8</sup> and CePdSb<sub>2</sub><sup>9</sup>. By examining the Pd-rich region, we remain in the vicinity of the canonical intermediate valent compound, CePd<sub>3</sub><sup>10</sup>, and hope to retain some similar aspects in the cerium environment and electronic behavior. We have previously found the ternaries Ce<sub>3</sub>Pd<sub>6</sub>Sb<sub>5</sub><sup>11</sup>, which is a ordered-defect variant of the CaBe<sub>2</sub>Ge<sub>2</sub> structure type, and Ce<sub>8</sub>Pd<sub>24</sub>Sb<sup>12</sup>, a distorted variant of Cu<sub>3</sub>Au and perovskite structures and very close in composition to CePd<sub>3</sub>. We now have the opportunity to examine a ternary, Ce<sub>2</sub>Pd<sub>9</sub>Sb<sub>3</sub>, high in palladium content yet relatively low in cerium content.

## **Experimental Details**

Starting materials for all samples were elements of at least 99.9 % purity ( Ce ingot, Ames; 1 mm diameter Pd wire, Strem; Sb shot, Cerac). An initial sample of composition "CePd<sub>3</sub>Sb" was prepared by arc-melting of the elements with a small (1 %) excess of the more

volatile antimony to compensate for anticipated loss. Final masses of arc-melted samples were within 0.5% of the expected mass. The 1:3:1 sample was determined to be multi-phase by powder diffraction and attempts to extract a crystal did not yield any suitable for study. An attempt to grow larger crystals from an equimolar flux of NaBr and KBr was made using 0.3365g of "CePd<sub>3</sub>Sb" and 0.6425g of flux. This mixture was placed in a vitreous carbon crucible (EMC Industries, type GAZ-02), sealed in an evacuated quartz tube and subjected to the following heating cycle: 1 day at 900°C, cool over 4 days to 700°C, 3 days at 700°C, then allowed to cool to room temperature. The product of this reaction, apart from numerous crystals of flux, was in the form of spherical nodules. Washing with distilled water, then acetone enabled the nodules to be isolated from most of the flux. When crushed, the nodules revealed themselves to have single crystalline interiors. Microprobe (EDAX using a JEOL733 Superprobe) results on fragments from crushed nodules, while indicating some trace (<4%) amounts of bromine on the surface of the nodules, showed invariably only cerium, palladium and antimony for material liberated from the interiors of nodules. The mean interior composition obtained was 13.9(4) at % Ce, 64.4(7) at % Pd and 20.9(5) at % Sb, consistent with a 2:9:3 stoichiometry. Given the form of the product, we do not believe the material dissolved in the flux. The flux may have acted to assist in phase separation of the 1:3:1 material on reaching the liquidus for this composition. Following the single crystal study, samples of 2:9:3 composition were prepared by arc-melting, placed in sections of tantalum tubing and sealed in evacuated quartz tubes for anneal. Samples were annealed for 4-5 weeks at 750°C.

Single crystals of Ce<sub>2</sub>Pd<sub>9</sub>Sb<sub>3</sub> were isolated from crushed nodules from the above reaction and examined by precession methods for suitability for single crystal data collection.

Single crystal data was collected on a P4 automatic 4-circle diffractometer using graphite monochromatised Mo K $\alpha$  radiation. Powder diffraction data were collected using a SCINTAG  $\theta/2\theta$  diffractometer using Cu K $\alpha 1$  radiation and Al<sub>2</sub>O<sub>3</sub> as an internal standard. Due to the hardness of the material, grinding at 300K (in an argon-filled glove box) resulted in severe strain-broadening of diffraction peaks. Grinding under liquid nitrogen enabled a powder dataset to be collected with peaks sufficiently resolved to be indexed using the program TREOR90<sup>13</sup>. For least-squares refinement of lattice parameters, material was ground and annealed for one week at 750°C (in tantalum and evacuated quartz). A theoretical powder pattern was calculated using the program XPOW<sup>14</sup> for comparison to powder diffraction data on annealed powder.

Magnetic measurements were performed by the Faraday method at a field of 11.6kG ( $H\partial H/\partial z = 10.97 \text{ kG}^2/\text{cm}$ ) on a single piece of Ce<sub>2</sub>Pd<sub>9</sub>Sb<sub>3</sub> (40.7(1) mg) isolated by cracking a larger bead under liquid nitrogen. Susceptibility data was fit<sup>3</sup> to a Curie-Weiss expression:

$$\chi = \chi_o + \frac{C}{(T-\theta)} \quad (1)$$

with  $\theta$  positive for ferromagnetic interactions. Resistivity measurements were performed by a four-probe technique by soldering indium contacts to a 13.8(1) x 3.9(1) x 3.7(1) mm<sup>3</sup> ingot.

## Results and Discussion

### *Crystal structure*

Precession photographs of a rectangular platelet isolated from the attempt at flux growth revealed a hexagonal sub-cell with superlattice spots suggesting a true symmetry of

orthorhombic. Insufficient supercell data prevented a space group determination from precession photographs other than to suggest C-centring. During the course of the single crystal data collection, the Laue group was determined to be mmm and during processing of the data using the program XPREP<sup>15</sup>, the space group Cmcm (no. 63) was selected.

Starting atomic positions were determined by direct methods using the program SIR92<sup>16</sup> and all F<sup>2</sup> data. Subsequent refinement of positions and thermal parameters was done using the program XL<sup>15</sup> with anisotropic thermal parameters for all atoms. A final difference Fourier synthesis revealed no significant residual peaks greater than +2.062 or -2.421 e/Å<sup>3</sup>. Details of the crystal data collection and refinement are given in Table 1. Refined atomic positions and interatomic distances based on single crystal data are given in Tables 2 and 3, respectively. Additional information on the refinement is available<sup>17</sup>. Refined lattice constants obtained from powder diffraction data on annealed powder are:  $a = 13.7623(9)\text{\AA}$ ,  $b = 8.0382(5)\text{\AA}$  and  $c = 9.3492(6)\text{\AA}$  based on 45 diffraction peaks with  $2\theta$  values ( $\lambda = 1.5406\text{\AA}$ ) ranging from 15 to 78 degrees, in good agreement with the single crystal values. A comparison of observed and calculated<sup>14</sup> powder diffraction patterns is given in Table 4.

The structure of Ce<sub>2</sub>Pd<sub>9</sub>Sb<sub>3</sub> (Fig. 1) is of the Y<sub>2</sub>Co<sub>3</sub>Ga<sub>9</sub> type<sup>18</sup> with palladium occupying the gallium positions and antimony, the cobalt positions in an anti-site fashion. The pseudo-hexagonal (trigonal) arrangement of antimony atoms is quite apparent in Figure 1, as is the pseudo-hexagonal array of cerium atoms. The cerium hexagonal network at  $z = 0.75$ , however, is shifted by  $0.5b$  relative to the array at  $z = 0.25$ . Near neighbour distances in Table 3 indicate no true hexagonal or trigonal symmetry since no atom has 3 equidistant neighbours. This structure type has been well-described in terms of an intergrowth of

hexagonal layers related to CoAl and  $\text{Th}_3\text{Pd}_5$  in structure<sup>20</sup> as the gallium<sup>18</sup> and aluminum<sup>20</sup> variants and the related  $\text{ErNi}_3\text{Al}_9$ <sup>21</sup> ternary compound.

Cerium atoms in  $\text{Ce}_2\text{Pd}_9\text{Sb}_3$  have one cerium neighbour at 4.256Å but the next two cerium atoms are 4.804Å away. This difference is much larger than in the  $\text{Y}_2\text{Co}_3\text{Ga}_9$  structure where each yttrium has one yttrium neighbour at 4.182Å and two more at 4.286Å. The 4.256Å separation is comparable to Ce-Ce distances in  $\text{Ce}_3\text{Pd}_6\text{Sb}_5$ <sup>11</sup> and in  $\text{Ce}_8\text{Pd}_{24}\text{Sb}$ <sup>12</sup> but the much larger 4.804Å distances indicates that any Ce-Ce interactions are likely to be limited to the pairs of cerium 4.256Å apart. Cerium-palladium distances range from 3.075Å (Ce-Pd(4)) to 3.323Å (Ce-Pd(3)) in the immediate cerium environment with the next Pd further away at a distance of 3.559Å. These distances are intermediate between those for  $\text{Ce}_8\text{Pd}_{24}\text{Sb}$  (2.975Å - 3.050Å) and  $\text{Ce}_3\text{Pd}_6\text{Sb}_5$  (3.269Å to 3.666Å). At 3.449Å (Ce-Sb1) and 3.577Å (Ce-Sb2), cerium - antimony distances in the 2:9:3 compound again lie between those for the 3:6:5 (3.290Å to 3.337Å) and 8:24:1 (3.684Å) compounds.

Strong Sb-Pd and Pd-Pd interaction is evident from the close interatomic distances within and *between* the pseudo-hexagonal layers. This suggests the presence of strong covalent bonds between these elements in  $\text{Ce}_2\text{Pd}_9\text{Sb}_3$ . The nearest neighbours to each antimony atom are palladium (Table 3) with 4 palladium atoms at distances comparable to or shorter than the sum of covalent radii<sup>21</sup>, 2.68Å. This is shown in figure 2 in a polyhedral representation. The shortest near neighbours to Sb1 are coplanar in rectangular sheets while the 4 palladium atoms closest to Sb2 are in a distorted tetrahedral geometry. These tetrahedra are linked end to end by short Pd4-Pd4 bonds which, at a distance of 2.710Å, are comparable to the Pd-Pd distance in palladium metal<sup>23</sup>, 2.751Å. The rectangular sheets for Sb1 are also linked with one Pd3

being shared between 2 antimony atoms at a distance of 2.614Å to provide a staggered chain propagating along *c* from the c-glide. The other corners of the sheet are linked by a close Pd2-Pd2 distance of 2.743Å. The set of close Pd-Pd contacts are grouped as elongated (along *c*) octahedra in figure 2. Four additional palladiums at distances slightly larger than the covalent radii sum co-ordinate each antimony and serve to connect the shorter bonded units into the larger structure. This interconnected covalent network of palladium and antimony is indicated by the Pd-Pd and Pd-Sb bonds included in Figure 1. The range of Sb-Pd bond lengths (2.593Å to 2.839Å) is much larger, as also noted above for the Ce-Ce distances, in  $\text{Ce}_2\text{Pd}_9\text{Sb}_3$  than in the series  $\text{Ln}_2\text{Co}_3\text{Ga}_9$ <sup>18</sup>. Even the neodymium version of the cobalt-gallide, which has the largest cell size (and largest rare earth) of the series, has Co-Ga distances<sup>24</sup> which vary only over the range 2.521Å to 2.591Å. With palladium and gallium comparable in size, we attribute the larger distortions away from pseudo-hexagonal symmetry to the much larger size of antimony compared to that of cobalt.

#### *Magnetic and Electric Behavior*

The inverse of the magnetic susceptibility of  $\text{Ce}_2\text{Pd}_9\text{Sb}_3$  (Fig. 3) is almost Curie-like in its temperature dependence. The susceptibility can be fit to a Curie-Weiss expression over the temperature range of 100K to 346K to yield an effective moment per cerium of 2.51(3) $\mu_B$ . The  $\theta$  parameter is small, 2(2)K, as is the temperature independent term,  $\chi_0$ , at  $-8(8)\times 10^{-8}$  emu/g. The inverse magnetic susceptibility deviates from linearity below 100K in the direction of increasing  $\chi^{-1}$  (decreasing slope of  $\chi^{-1}$  vs. T). This deviation may arise from some temperature dependence of the cerium moments since the population of the levels in a crystal-

field-split cerium 4f state will vary when the temperature is on the order of the field splitting<sup>3</sup>. A decreasing slope of  $\chi^{-1}$  versus temperature may also arise from an interaction which can screen a moment, if present, like the Kondo effect associated with heavy fermion behavior<sup>1</sup>. No ordering is observed above 4.2K. The absence of long range order can be understood by the relative isolation of the cerium atoms. With one cerium neighbour 4.256Å away and 2 others much further at 4.804Å, any magnetic interaction is likely dominated by the pair 4.256Å apart. The RKKY interaction<sup>25</sup>, which can lead to magnetic order if no direct exchange between moments is present, decreases as (separation)<sup>-3</sup> and varies periodically as  $(2k_{\text{Fermi}})^{-1}$  so only weak Ce-Ce interactions may occur if the Ce-Ce distance becomes large or if the cerium separation coincides with a node in the RKKY-induced modulation of the conduction electron spins.

The resistivity of  $\text{Ce}_2\text{Pd}_9\text{Sb}_3$  (Fig. 4) is unusual for a trivalent-cerium compound. Above 50K, the resistivity is almost linear, as if it were a simple metal<sup>25</sup>. Below 30K, the resistivity again appears almost linear, with decreased slope, but does not plateau as observed in simple metals due to scattering by defects and impurities. If some interaction of conduction electrons with cerium f-states split by a crystal field were present, then one typically sees a reduction in magnetic scattering (an increasing slope with decreasing temperature from depopulation of crystal-field levels) over a broad range of temperature as is observed<sup>11</sup>, for example, in  $\text{Ce}_3\text{Pd}_6\text{Sb}_5$  between 50K and 100K. In  $\text{Ce}_2\text{Pd}_9\text{Sb}_3$ , there does not appear to be an appreciable interaction between the cerium moments and conduction electrons.

## **Conclusions**

We have examined the crystal structure and physical properties of a new ternary compound,  $\text{Ce}_2\text{Pd}_9\text{Sb}_3$ . The orthorhombic crystal structure is related to the known  $\text{Y}_2\text{Co}_3\text{Ga}_9$  structure by an anti-site relationship between the transition and p-block elements. The larger size of antimony compared to cobalt has produced larger distortions away from the pseudo-trigonal symmetry in the parent structure type. The magnetic susceptibility exhibits Curie behavior with an effective high temperature cerium moment of  $2.51(3)\mu_B$ . Neither the susceptibility nor the resistivity give any indication of significant interaction between conduction electrons and the cerium moments.

## **Acknowledgements**

We would like to thank Prof. Dr. A. Simon for the use of the facilities at the MPI. This work was supported by the Office of Naval Research and the Stiftung Stipendienfonds des Verbandes der Chemischen Industrie by a Liebig grant to R.P.

## References

1. F. Steglich, C. Geibel, K. Gloos, G. Olesch, C. Schank, C. Wassilew, A. Loidl, A. Krimmel and G.R. Stewart, *J. Low Temp. Phys.*, 1994, **93**, 3.
2. D.T. Adroja and S.K. Malik, *J. Magn. Magn. Mater.*, 1991, **100**, 126.
3. R.A. Gordon, Y. Ijiri, C.M. Spencer and F.J. DiSalvo, *J. Alloys Comp.*, 1995, **224**, 101.
4. R. Pöttgen, *J. Mater. Chem.*, 1995, **5**, 505.
5. R. Pöttgen, H. Borrmann and R. K. Kremer, *J. Magn. Magn. Mater.*, in press.
6. R. Pöttgen, H. Borrmann, C. Felser, O. Jespen, R. Henn, R.K. Kremer and A. Simon, *J. Alloys Comp.*, submitted.
7. R. Marazza, D. Rossi and R. Ferro, *J. Less-Common Met.*, 1980, **75**, P25.
8. W.K. Hofmann and W. Jeitschko, *Monatsh. Chem.*, 1985, **116**, 569.
9. O. Sologub, K. Hiebl, P. Rogl, H. Noël and O. Bodak, *J. Alloys Comp.*, 1994, **210**, 153.
10. H. Sthioul, D. Jaccard and J. Sierro, in *Valence Instabilities*, eds. P. Wachter and H. Boppart, North-Holland, 1982, p. 443.
11. R.A. Gordon, F.J. DiSalvo and R. Pöttgen, *J. Alloys Comp.*, 1995, **228**, 16.
12. R.A. Gordon and F.J. DiSalvo, *Z. Naturforsch. B*, in press.
13. P.E. Werner, L. Eriksson and M. Westdahl, *J. Appl. Crystallogr.*, 1985, **18**, 367.
14. R.T. Downs, K. L. Bartelmehs, G.V. Gibbs and M.B. Boisen Jr., *Am. Mineral.*, 1993, **78**, 1104.
15. G.M. Sheldrick, SHELLXTL PC Version 5.0 - An Integrated System for Solving, Refining and Displaying Crystal Structures from Diffraction Data, Siemens Analytical X-Ray Instruments Inc., Madison, WI, 1994.

16. A. Altomare, G. Cascarano, C. Giacovazzo and A. Guagliardi, *J. Appl. Crystallogr.*, 1994, **27**, 435.
17. Details may be obtained from Fachinformationszentrum Karlsruhe, D-76344 Eggenstein-Leopoldshafen, Germany, by citing the registry number, CSD #####, the journal citation and names of the authors.
18. Yu.N. Grin, R.E. Gladyshevskii, O.M. Sichevich, V.E. Zavodnik, Ya.P. Yarmolyuk and I.V. Rozhdestvenskaya, *Sov. Phys. Crystallogr.*, 1984, **29**, 528.
19. E. Dowty, ATOMS for Windows Version 3.1 ( $\beta$ 3), Shape Software, Kingsport TN, 1994.
20. R.E. Gladyshevskii, K. Cenzual and E. Parthé, *J. Alloys Comp.*, 1992, **182**, 165.
21. R.E. Gladyshevskii, K. Cenzual, H.D. Flack and E. Parthé, *Acta Cryst.*, 1993, **B49**, 468.
22. R.T. Sanderson, *Inorganic Chemistry*, Reinhold Publishing Corporation, 1967, 74.
23. J. Donohue, *The Structures of the Elements*, Wiley, New York, 1974, 216.
24. Calculated based on the positions of  $\text{Ho}_2\text{Co}_3\text{Ga}_9$  in reference 17.
25. J.M Ziman, *Principles of the Theory of Solids* (2nd Edition), Cambridge, 1972, chapters 7&10.

**Table 1**  
Crystal and structure refinement data for  $\text{Ce}_2\text{Pd}_9\text{Sb}_3$

Empirical formula	$\text{Ce}_2\text{Pd}_9\text{Sb}_3$
Formula weight	1603.09
Temperature	293(2) K
Wavelength	0.71069 Å
Crystal system	Orthorhombic
Space group	Cmcm (No. 63)
Unit cell dimensions	a = 13.769(2) Å b = 8.0412(8) Å c = 9.3482(10) Å
Volume, Formula units	1035.0(2) Å <sup>3</sup> , 4
Density (calculated)	10.288 g/cm <sup>3</sup>
Absorption co-efficient	31.419 mm <sup>-1</sup>
F(000)	2732
Crystal size	0.151 x 0.094 x 0.019 mm <sup>3</sup>
Theta range for data collection	2.93° to 30.00°
Limiting indices	-6 ≤ h ≤ 14, -4 ≤ k ≤ 10, -10 ≤ l ≤ 4
Reflections collected	2064
Independent reflections	709 [R <sub>int</sub> = 0.0640]
Reflections with I > 2σ(I)	586 [R <sub>o</sub> = 0.0546]
Absorption correction	From ψ-scan data
Max. and min. transmission	0.652 and 0.288
Refinement method	Full-matrix least-squares on F <sup>2</sup>
Data / restraints / parameters	709 / 0 / 42
Goodness-of-fit on F <sup>2</sup>	1.039
SIR92 R index (all data)	R <sub>SIR</sub> = 0.0646
Final R indices [I > 2σ(I)]	R <sub>1</sub> = 0.0300, wR <sub>2</sub> = 0.0631
R indices (all data)	R <sub>1</sub> = 0.0415, wR <sub>2</sub> = 0.0669
Extinction coefficient	0.00089(4)
Largest diff. peak and hole	2.062 and -2.421 e/Å <sup>3</sup>

**Table 2**

Atomic co-ordinates and isotropic displacement parameters ( $\text{pm}^2$ ) for  $\text{Ce}_2\text{Pd}_9\text{Sb}_3$  with  $U_{\text{eq}}$  defined as one third the trace of the  $U_{ij}$  tensor.

Wyckoff					
Atom	site	x	y	z	$U_{\text{eq}}$
Ce	8g	0.34547(6)	0.32828(8)	0.25	98(2)
Pd1	16h	0.17109(5)	0.17061(8)	0.08478(8)	110(2)
Pd2	8f	0	0.3323(1)	0.5268(1)	110(3)
Pd3	4c	0	0.1457(2)	0.25	92(3)
Pd4	8g	0.09840(8)	0.4582(1)	0.25	125(3)
Sb1	4a	0	0	0	81(3)
Sb2	8e	0.32369(6)	0	0	87(2)

**Table 3**

Single crystal interatomic distances (in Å) up to 4.8Å for cerium and 3.8Å for all other atoms. Standard deviations are all equal to or less than 0.002Å.

Ce:	1	Pd4	3.075	Sb2:	2	Pd4	2.593
	2	Pd1	3.124		2	Pd1	2.632
	2	Pd1	3.138		2	Pd1	2.766
	2	Pd1	3.165		2	Pd2	2.788
	2	Pd2	3.248		2	Ce	3.538
	1	Pd3	3.323		2	Ce	3.577
	2	Sb1	3.449				
	1	Pd4	3.559	Pd2:	1	Sb1	2.684
	2	Sb2	3.577		1	Pd2	2.743
	1	Ce	4.256		2	Sb2	2.788
	1	Pd4	4.581		2	Pd1	2.886
	2	Ce	4.804		1	Pd3	2.992
					2	Pd4	3.004
Pd1:	1	Sb2	2.632		2	Pd4	3.091
	1	Sb2	2.766		2	Ce	3.248
	1	Pd3	2.824				
	1	Sb1	2.839	Pd3:	2	Sb1	2.614
	1	Pd2	2.886		4	Pd1	2.824
	1	Pd4	2.956		2	Pd4	2.855
	1	Pd1	2.977		2	Pd2	2.992
	1	Pd1	3.089		2	Ce	3.323
	1	Ce	3.124				
	1	Ce	3.138	Pd4:	2	Sb2	2.593
	1	Ce	3.165		1	Pd4	2.710
	1	Pd1	3.169		1	Pd3	2.855
					2	Pd1	2.956
Sb1:	2	Pd3	2.614		2	Pd2	3.004
	2	Pd2	2.684		1	Ce	3.075
	4	Pd1	2.839		2	Pd2	3.091
	4	Ce	3.449		1	Ce	3.559

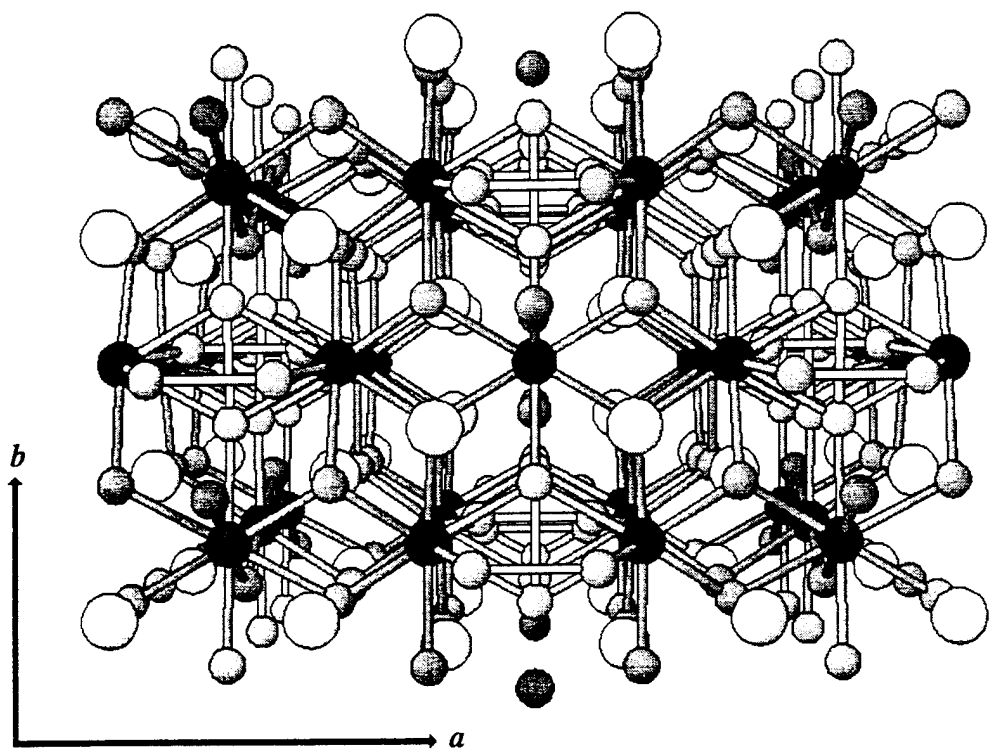
**Table 4**

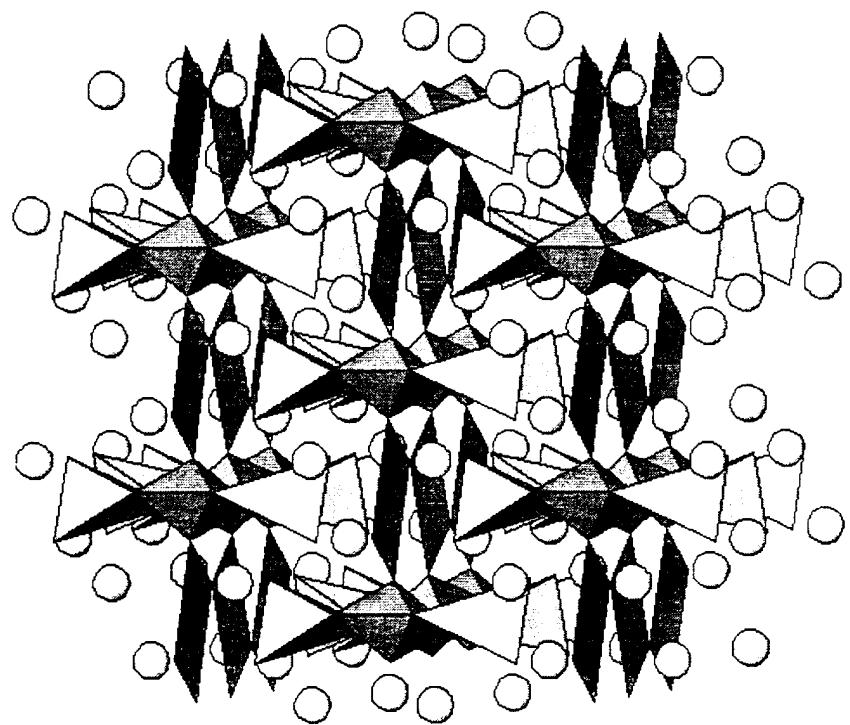
Comparison of calculated and observed diffraction lines for  $\text{Ce}_2\text{Pd}_9\text{Sb}_3$ . For unresolved peaks, intensity was assigned to the most intense peak of the set. Overlap of the (223) and (330) peaks has been considered by a rescaling of intensities ( $1.09 \times I_{\text{obs}}$ ) by the calculated sum.

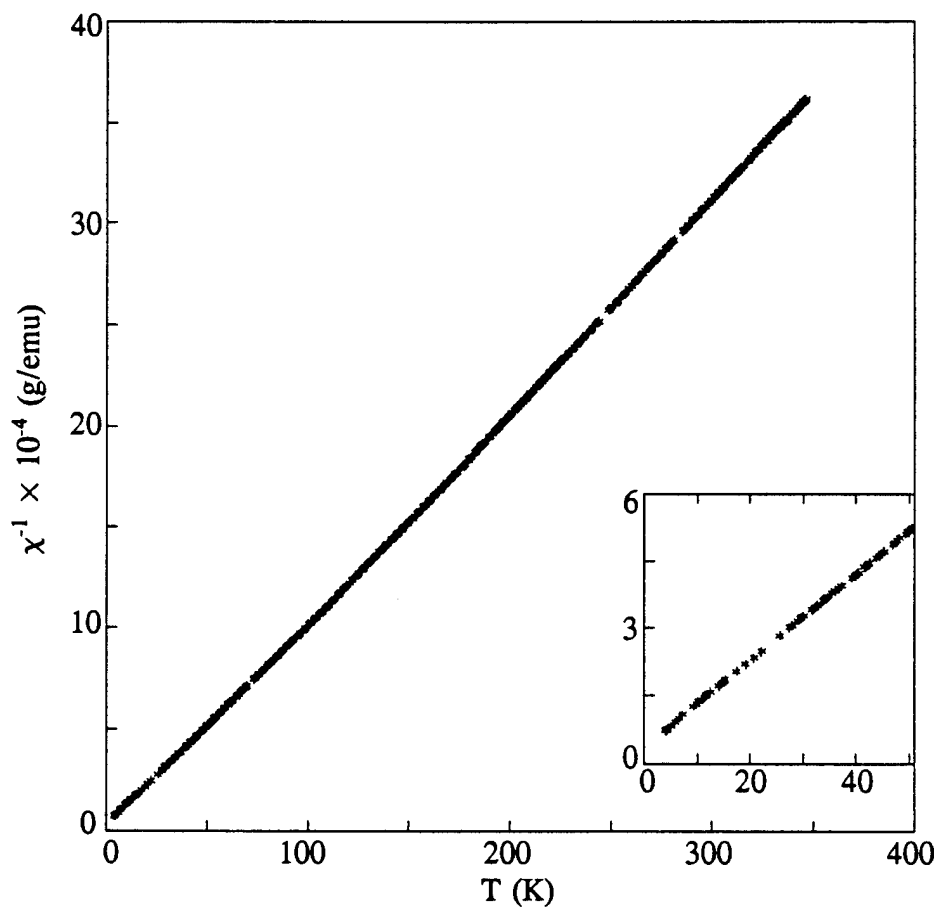
$h$	$k$	$l$	$d_{\text{calc}}$	$I_{\text{calc}}$	$I_{\text{obs}}$	$I_{\text{obs}} \times 1.09$	$h$	$k$	$l$	$d_{\text{calc}}$	$I_{\text{calc}}$	$I_{\text{obs}}$	$I_{\text{obs}} \times 1.09$
1	1	0	6.941	1	1	1.1	0	4	2	1.846	2.3	2	2.2
2	0	0	6.881	0.8			6	2	2	1.833	12.5	12	13.1
1	1	1	5.573	5.2	5	5.5	7	1	2	1.768	2.8	2	2.2
0	0	2	4.675	7.8	6	6.6	4	2	4	1.742	1.2	1	1.1
3	1	1	3.665	2.7	2	2.2	0	4	3	1.689	5.5	4	4.4
2	2	0	3.471	1.5	<1		6	2	3	1.679	9.1	7	7.6
4	0	0	3.441	2.8	2	2.2	2	2	5	1.646	1.6		
2	2	1	3.256	2.3	1	1.1	3	3	4	1.644	10.4	10	10.9
0	2	2	3.048	2.4	3	3.3	2	4	3	1.640	4.4	6	6.5
3	1	2	3.032	6.7	6	6.5	6	0	4	1.637	4.2		
1	1	3	2.843	2.1	1	1.1	7	1	3	1.628	1.2	<1	
2	2	2	2.787	5.7	6	6.5	0	0	6	1.558	2.5	1	1.1
4	0	2	2.771	22.2	21	22.9	0	4	4	1.524	1.3	<1	
1	3	0	2.630	12.6	13	14.2	4	2	5	1.521	5.5	4	4.4
5	1	0	2.604	6.6	8	8.7	7	3	2	1.501	7.5	6	6.5
1	3	1	2.532	5.6	9	9.8	5	3	4	1.484	2.0	1	1.1
4	2	1	2.517	17.3	18	19.6	7	1	4	1.479	1.5	1	1.1
5	1	1	2.509	1.3			0	2	6	1.453	3.6		
0	2	3	2.463	38.8	31	34.2	3	1	6	1.451	6.6	5	5.5
3	1	3	2.455	98.4	84	91.8	3	5	2	1.443	2.1	1	1.1
0	0	4	2.337	28.2	22	24.0	6	4	2	1.438	4.9	4	4.4
2	2	3	2.319	9.3			9	1	2	1.430	2.5	1	1.1
3	3	0	2.314	100.0	100	109.3	2	2	6	1.422	2.1		
6	0	0	2.294	44.6	61	66.7	1	5	3	1.421	1.5		
1	3	2	2.292	32.4			4	0	6	1.419	4.2	4	4.4
5	1	2	2.275	19.8	29	31.7	8	0	4	1.386	1.9	1	1.1
1	1	4	2.215	3.0			10	0	0	1.376	0.6	1	1.1
2	0	4	2.213	7.6	8	8.7	5	5	1	1.373	2.7	1	1.1
3	3	2	2.074	31.5	25	27.3	3	5	3	1.364	12.7	10	10.9
6	0	2	2.059	16.6	17	18.6	6	4	3	1.360	12.7	10	10.9
0	2	4	2.021	7.5	5	5.5	9	1	3	1.353	11.3	9	9.8
3	1	4	2.016	13.1	12	13.1	1	3	6	1.341	9.2	15	16.4
1	3	3	2.010	3.3	3	3.3	0	6	0	1.340	8.4		
4	2	3	2.003	14.2	11	12.0	5	1	6	1.337	5.3	4	4.4
5	1	3	1.998	1.8	2	2.2	9	3	0	1.328	8.2	6	6.5
6	2	0	1.992	4.1	3	3.3	1	1	7	1.312	1.3	<1	
0	4	1	1.965	2.1	2	2.2	0	6	2	1.288	1.6	1	1.1
6	2	1	1.948	3.5	2	2.2	9	3	2	1.278	8.8	6	6.5
7	1	0	1.910	3.5	2	2.2	0	4	6	1.231	2.2	2	2.2
2	4	1	1.889	1.1	<1		6	2	6	1.227	9.3	6	6.5

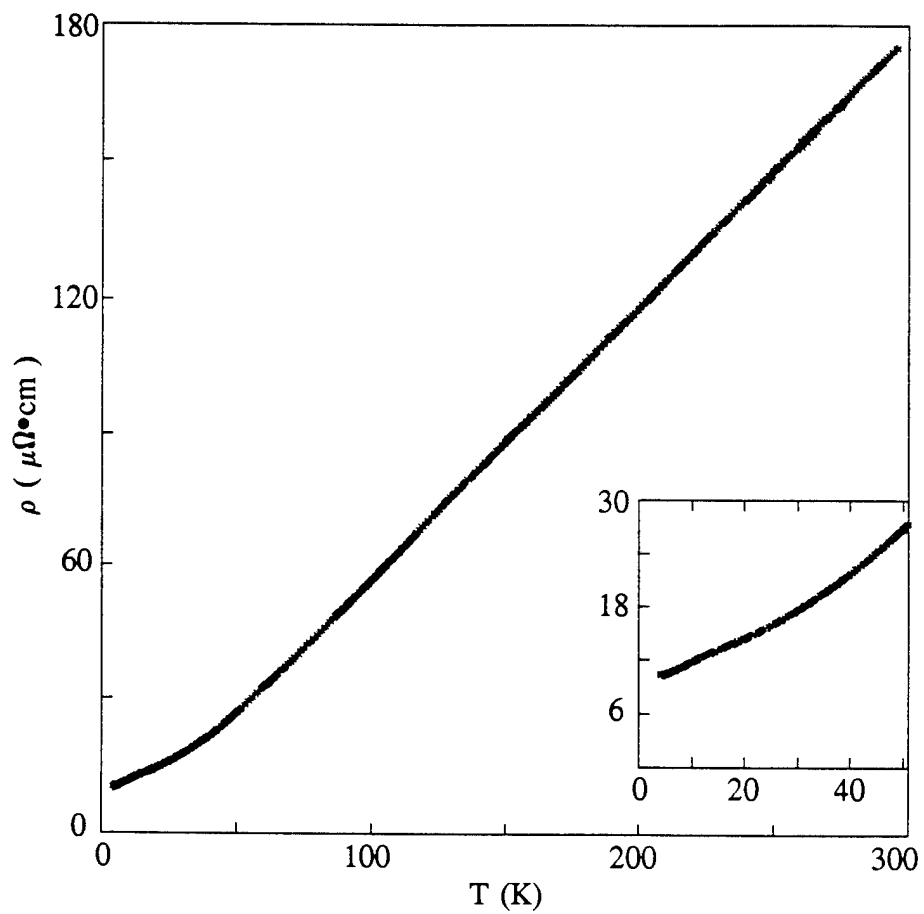
## Figure captions

- Fig. 1. Perspective view of the unit cell of  $\text{Ce}_2\text{Pd}_9\text{Sb}_3$  showing Pd-Pd and Pd-Sb bonding<sup>19</sup>. The view is down the c-axis with near-neighbour atoms from adjoining cells. Atom designations are: large white spheres, Ce; small gray spheres, Pd; medium dark spheres, Sb.
- Fig. 2. Polyhedral representation of the shortest Sb-Pd and Pd-Pd contacts. Rectangular sheets and distorted tetrahedra are centred by Sb(1) and Sb(2) respectively. Elongated  $\text{Pd}_6$  octahedra are also present joining the tetrahedra.
- Fig. 3. Inverse magnetic susceptibility of  $\text{Ce}_2\text{Pd}_9\text{Sb}_3$  from 4.2K to 346K. Shown in inset are data from 4.2K to 50K.
- Fig. 4. Resistivity of  $\text{Ce}_2\text{Pd}_9\text{Sb}_3$  from 4.2K to 295K.









Technical Report Distribution List

Dr. John C. Pazik (1)\*  
Physical S&T Division - ONR 331  
Office of Naval Research

800 N. Quincy St.  
Arlington, VA 22217-5660

Defense Technical Information  
Ctr (2)  
Building 5, Cameron Station  
Alexandria, VA 22314

Chemistry Division, Code 385  
NAWCWD - China Lake  
China Lake, CA 93555-6001

Dr. James S. Murday  
(1)  
Chemistry Division, NRL 6100  
Naval Research Laboratory  
Washington, DC 20375-5660

Dr. Peter Seligman (1)  
NCCOSC - NRAD  
San Diego, CA 92152-5000

Dr. John Fischer (1)

Dr. Bernard E. Douda (1)  
Crane Division  
NAWC  
Crane, Indiana 47522-5000

\* Number of copies required